Crystal growth / Croissance cristalline

Colloidal properties of biomacromolecular solutions: Towards urate oxidase crystal design

Propriétés colloïdales de solutions de macromolécules biologiques : Applications à la croissance cristalline de l'urate oxydase

Françoise Bonneté

Institut des biomolécules Max-Mousseron, IBMM UMR 5247, faculté des sciences d'Avignon, 33, rue Louis-Pasteur, 84000 Avignon, France

A B S T R A C T

Crystallization of biological macromolecules is governed by weak interaction forces, attractive and repulsive. Knowledge of solution properties, via second virial coefficient measurements, makes it possible to select physico-chemical parameters that govern and control phase diagrams and thus to grow crystals for specific applications (bio-crystallography or pharmaceutical processes). We highlight here with urate oxidase a salting-in effect that increases its solubility and the depletion effect of amphiphilic polymer, at a polymer concentration above its cmc, in order to grow diffracting crystals of urate oxidase. These two effects were used to grow crystals for high pressure crystallography and in a purification process.

© 2013 Académie des sciences. Published by Elsevier Masson SAS. All rights reserved.

R É S U M É

La cristallisation des macromolécules biologiques est gouvernée par un équilibre d'interactions faibles, attractives et répulsives. La connaissance des propriétés des solutions, via la mesure du second coefficient du virial, nous permet de choisir les paramètres physico-chimiques qui gouvernent ces potentiels et de contrôler les diagrammes de phases et ainsi croître des cristaux pour des applications spécifiques de la bio-cristallographie au procédé industriel. Nous avons mis en évidence, avec l'urate oxydase, un effet *salting-in* qui augmente sa solubilité ainsi que l'effet de déplétion d'un polymère amphiphile permettant de cristalliser la protéine à une concentration en polymère supérieure à sa cmc. Ces deux effets ont été utilisés pour croître des cristaux pour la diffraction des rayons X sous pression ainsi que pour purifier la protéine par cristallisation.

© 2013 Académie des sciences. Published by Elsevier Masson SAS. All rights reserved.

1. Introduction

Crystallization in solution is a physical liquid–solid interfacial process mainly used (1) in bio-crystallography to decipher biological macromolecule 3D-atomic structures and understand their structure-function relationship, (2) in chemistry as a method of purification and (3) in pharmaceutical processing as a means to design bioavailable drug polymorphs. Although valuable in many fields, crystallization of biomolecules remains an empirical process, still based on trial-and-error methods.

For example, proteins, which are composed of various numbers of different amino acids leading to various folded structures of different shapes and different sizes, can be considered by physicists as colloids with an effective charge in a continuous solvent containing ions and/or polymers. These charged colloids interact in the solvent through weak interaction forces including hard-sphere, electrostatic, van der Waals, depletion potentials. It is usual in the colloid field to calculate phase diagrams from interaction potentials in solution [1], the range of these forces modifying the appearance of the phase diagram [2]. This is more difficult with proteins, since in addition to the usual colloidal forces, less defined forces (hydrophobic, hydration, etc.) may play a role and biological macromolecules can be sensitive to physico-chemical parameters, which may modify their stability and structural conformation. Even though it is not yet possible to calculate stricto sensu interaction potentials from macromolecule characteristics, the "colloidal" approach can be applied to guide crystallization of stable proteins [3,4]. It is thus possible both to measure resulting interactions in solution, either repulsive or attractive, through second virial coefficient (A_2) measurements and then to simulate the underlying pair potentials. A_2 is determined from the macromolecule concentration dependence of different experimental measurements, such as osmotic pressure, analytical ultracentrifugation, self-interaction chromatography, static light scattering, small angle X-ray or neutron scattering (SAXS or SANS). In the 1990s, A_2 appeared to be a powerful tool for predicting crystallization conditions of proteins. Several authors showed that a restrictive range of negative values of the second virial coefficient was favorable to crystallization of soluble proteins [5–7]. This "crystallization slot", which is about $[-1 \times 10^{-4}; -8 \times 10^{-4} \ \mathrm{mol\,mL\,g^{-2}}]$, corresponds to slight or moderate attractions. However, while A_2 appears to be an indicator of the "crystallizability" of macromolecules, it does not give any indication of how potentials between macromolecules vary with physico-chemical parameters. By combining SAXS measurements and numerical simulations, we were able to analyze the different repulsive and attractive forces present in macromolecule solutions and study them as a function of usual physico-chemical parameters (pH, ionic strength, percentage of polymer, etc.). As a result, predicting the phase diagram — usually represented by the solubility curve — in the case of proteins based on knowledge of interaction forces may appear a more effective alternative for controlled crystallization than the usual trial-and-error screenings.

The literature, to which we have contributed significantly, substantially confirms that it is the repulsive or the attractive character of these interactions which either favors solubility or transparency [8] of macromolecule solutions or induces a variety of phase transitions [9,10], including macromolecular crystallization [11,12]. The repulsive regime is usually due to electrostatic potential, whereas the attractive regime is induced by addition of salt or polymer. Each potential was described via different model proteins: hen egg white lysozyme as a function of pH, salt concentration, salt type and temperature [3], alpha crystallins [13], aspartate transcarbamylase [14] and urate oxidase [4] as a function of polyethylene glycol (PEG). It was thus shown that, whatever the salt or polymer used, macromolecular crystallization occurs in the presence of an attractive pair potential, which depends on the size of the macromolecule. With low molecular weight proteins, a coulombic, pH-dependent, repulsive potential plus a short-range van der Waals attraction are sufficient to account for the behavior observed at low ionic strengths. At higher ionic strengths, salts following the (direct or reverse) order of the Hofmeister series induce an additional short-range salt-specific attraction, which can induce crystallization. With increasing protein size, the van der Waals contribution becomes negligible. As described by Asakura and Oosawa [15], adding polymers like polyethylene glycol (PEG) can aid crystallization by inducing a depletion attraction. While depletion potential depth increases with polymer concentration whatever the polymer size, depletion range is approximately equal to $2R_g$ for each polymer, whatever its concentration. Crystallization in polyethylene glycol is thus induced by a medium-range attractive potential between macromolecules. Recently, we have observed new molecular effects (ion binding, amphiphilic effect), which show interesting interactive effects in the control of phase diagrams and crystal growth.

In this article, we will therefore show how to select physico-chemical parameters to modulate the different interaction forces and design appropriate phase diagrams for specific applications (bio-crystallography or pharmaceutical processes for example) in the special case of urate oxidase. In the experimental section we will first describe how measuring second virial coefficients allows us to determine urate oxidase solubility and how characterizing the different underlying pair potentials makes it possible to control solubility and phase diagram by an appropriate balance between repulsion and attraction. Then in the results section, we will describe two new effects, ion binding and amphiphilic effect for specific applications, a high pressure crystallography experiment and a purification process.

2. Theoretical and experimental basis

2.1. Small angle X-ray scattering and interaction potentials

Often used to determine the shape of particles in solution, Small Angle X-Ray Scattering (SAXS) is a particularly suitable technique to characterize weak interaction forces between particles in solution. Indeed, the total normalized intensity $I(c, q)$, scattered by a solution of monodisperse particles at a scattering angle 2θ, can be expressed as a function of the particle concentration c and the modulus of the scattering vector q, $q = 4\pi\lambda^{-1}\sin\theta$ by the following expression:

$$I(c, q) = I(0, q) \times S(c, q) \tag{1}$$

$I(0, q)$ is the intensity scattered by one particle and is usually called the particle form factor. $S(c, q)$, usually called the solution structure factor, reflects spatial correlations and therefore interaction potentials between particles (ex. Fig. 1).
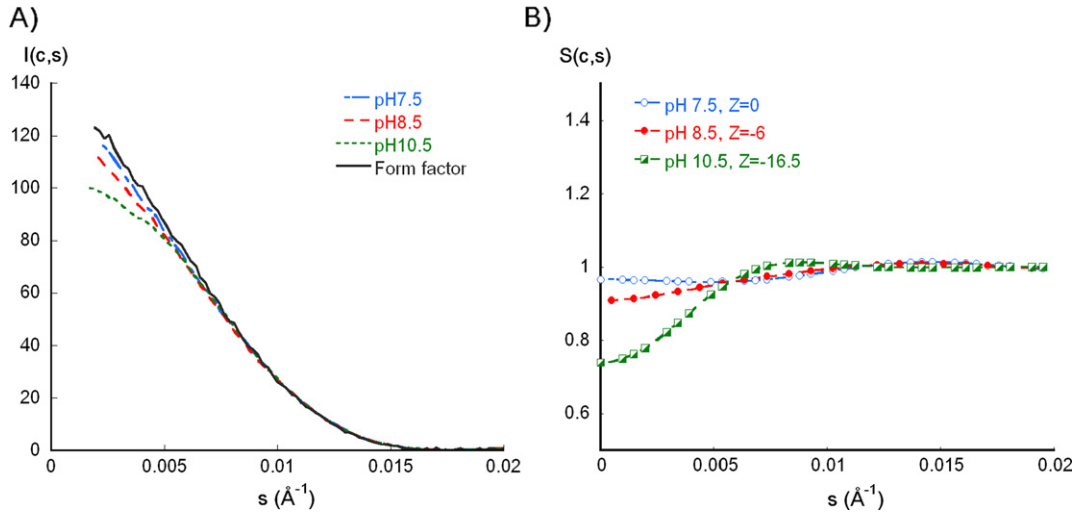
Fig. 1. A) Scattering intensities of urate oxidase as a function of pH. The form factor (black line) represents the solution of urate oxidase without interactions. B) Experimental (dots) and fitted (lines) repulsive structure factor of urate oxidase at different pH corresponding to repulsive interactions, $S(c, 0) < 1$ (Z is the net charge of urate oxidase).

Experimentally, the form factor is obtained from curves recorded at low concentrations to avoid interaction effects at high concentrations. The form factor gives information on the particle shape and its oligomeric state. At low angles, the form factor of an ideal solution of monodisperse globular particles (i.e. without interaction) can be written as:

$$I(c \to 0, q) = I(c \to 0, 0) . \exp\left(-\frac{R_g^2}{3}q^2\right) \tag{2}$$

A "Guinier plot", i.e. a $\operatorname{Ln} I(q)$ plot versus q^2 [16], provides with intensity at the origin, $I(0, 0)$ and then with the structure factor at the origin, $S(c, 0)$, since $S(c, 0) = I(c, 0)/I(0, 0)$. The value of $S(c, q)$ at zero-q angle gives information on the nature of net interactions between particles via the second virial coefficient measurement (A_2). Indeed, A_2 depends on the interaction pair potential $U(r)$ between particles in solution [17] by the expression:

$$A_2 = \frac{2\pi N_a}{M^2} \int_0^\infty \left(1 - \exp\left(-\frac{U(r)}{k_B T}\right)\right).r^2 \, dr \tag{3}$$

with $U(r) = +\infty$ for $r < \sigma$, where r is the interparticle distance and σ the particle diameter.

The second virial coefficient (A_2) is determined by the plot of the structure factor at the origin, $S(c, 0)$, as a function of particle concentration, since it is related to the osmotic pressure Π [18] by:

$$S(c, 0) = \frac{RT}{M}\left(\frac{\partial \Pi}{\partial c}\right)^{-1} \tag{4}$$

with

$$\frac{\Pi}{cRT} = \frac{1}{M} + A_2 c + A_3 c^2 + \cdots \tag{5}$$

where c is the concentration expressed in $\mathrm{g\,cm^{-3}}$.

Therefore, the second virial coefficient can be obtained by the expression:

$$S(c, 0) = \frac{I(c, 0)}{I(0, 0)} = \frac{1}{1 + 2.M.A_2.c + \cdots} \tag{6}$$

The slope of the linear fit gives the coefficient A_2 in $\mathrm{mol\,ml\,g^{-2}}$.

$$S(c, 0) \approx 1 - 2.M.A_2.c \tag{7}$$

With repulsive interactions, the particles are evenly distributed and $S(c, 0)$ is lower than 1 (example Fig. 1B). With attractive interactions, fluctuations in particle distribution are observed and $S(c, 0)$ is larger than 1. If $S(c, 0)$ is lower than 1 (respectively larger than 1), A_2 is positive (respectively negative), and the overall interactions are repulsive (respectively attractive). The correlation between variations of both solubility and second virial coefficient shown with lysozyme [5] as well as the theoretical relation described between A_2 and solubility [19], prove that interactions between macromolecules are a useful

indicator of crystallization conditions. However to modify solubility and phase diagram with physico-chemical parameters, it is necessary to thoroughly describe the underlying potentials, which involves the analysis of the structure factor $S(c, q)$ over the total q-range.

The structure factor $S(c, q)$ is the Fourier transform of the spherically averaged auto-correlation function $g(r)$ of the particle distribution or pair-distribution function:

$$S(c, q) = 1 + \rho \int 4\pi r^2 \big(g(r) - 1\big) \frac{\sin rq}{rq} \, dr \tag{8}$$

where $\rho = cN_a/M$ is the number density of particles, i.e. the number of particles per unit volume and c the particle concentration in $\mathrm{g\,cm^{-3}}$.

Calculation of simulated structure factors is based on models of particle pair potential $U(r)$, from which a particle distribution $g(r)$ at equilibrium is inferred. The calculation of $g(r)$ is based on the Ornstein–Zernike (OZ) equation and on the hypernetted chain (HNC) integral equation and uses an iterative method [20,21]. The method has been thoroughly described in the case of one-component or two-component fluids [3,4,13] and will not be extensively described here. For the simplest "one-component" model, only the interaction pair potentials between macromolecules, which interact through solvent and ions, are explicitly considered in the numerical simulations. The potentials, either attractive or repulsive, are described with a Yukawa potential, which is a function of three parameters, the hard-sphere diameter of the particle, σ, the depth (strength), J, and the range, d, of pair potentials according to:

$$U(r)/k_B T = J(\sigma/r) \exp\big[-(r - \sigma)/d\big] \tag{9}$$

In the case of binary mixtures of macromolecules (mac) and polymers (pol), i.e. of "two-component" systems, the total scattered intensity, $I(c_i, c_j, q)$, can be expressed as a function of each component concentrations c_i by [22]:

$$I(c_i, c_j, q) = \Sigma_i \Sigma_j \sqrt{c_i c_j} \sqrt{I_i(0, q) I_j(0, q)} S_{ij}(q)$$
$$= I_{\mathrm{mac}}(c_{\mathrm{mac}}, q) + I_{\mathrm{mac\text{-}pol}}(c_{\mathrm{mac}}, c_{\mathrm{pol}}, q) + I_{\mathrm{pol}}(c_{\mathrm{pol}}, q) \tag{10}$$

Partial structure factors $S_{ij}(q)$ are related to the Fourier transform of partial pair distribution function $g_{ij}(r)$:

$$S_{ij}(q) = \delta_{\iota\varphi} + \sqrt{c_i c_j} \int \big(g_{ij}(r) - 1\big). \exp(irq) \, dr \tag{11}$$

where $i, j = 1, 2$, δ_{ij} is the Kronecker symbol ($\delta_{ij} = 0$ when $i \neq j$ and $\delta_{ij} = 1$ when $i = j$) and r the interparticle distance. To determine the pair distribution function, the usual procedure, as for one-component systems, is to use the Ornstein–Zernike equation to link the total, $h_{ij}(r) = g_{ij}(r) - 1$, and the direct, correlation $c_{ij}(r)$ functions. The closure equation is once again the HNC equation. From a set of the three direct potentials, $U_{\mathrm{pol\text{-}pol}}(r)$, $U_{\mathrm{mac\text{-}pol}}(r)$ and $U_{\mathrm{mac\text{-}mac}}(r)$, the theoretical scattered intensity from the binary mixture can be calculated and compared to the experimental scattering curve [4].

2.2. The DLVO model

For the sake of simplicity and because it accounts well for experimental results [3], the direct protein–protein potential was chosen equal to the DLVO potential. The DLVO potential is the sum of three potentials: a hard-sphere potential, an electrostatic repulsion and a van der Waals attraction. The hard-sphere potential reflects the fact that proteins cannot interpenetrate, the repulsive coulombic potential is due to the fact that each protein holds the same net charge and the van der Waals attractive potential is the resulting dispersion interaction between proteins. The respective mathematical expressions of the three potentials are:

– Hard-sphere potential:

$$U(r) = \begin{cases} +\infty & r \leqslant \sigma, \text{ with } \sigma \text{ the protein diameter} \\ 0 & r > \sigma \end{cases} \tag{12}$$

– Repulsive coulombic potential:

$$U^{\mathrm{coul}}(r) = Z^2 L_B / \big[\sigma(1 + 0.5\sigma/\lambda_D)^2\big].(\sigma/r).\exp\big(-(r - \sigma)/\lambda_D\big) \quad r > \sigma \tag{13}$$

with Z the effective protein charge, L_B the Bjerrum length (equal to $e^2/(4\pi\varepsilon_0\varepsilon_s k_B T) = 7.31$ Å at $T = 293.15$ K with $\varepsilon_\sigma = \varepsilon_{\mathrm{H_2O}} = 80$) and λ_D the Debye length ($\lambda_D(\text{Å}) = 3/\sqrt{I}$ at 293.15 K where I is the ionic strength expressed in mol/l). The potential is expressed in $k_B T$ units.

– van der Waals potential:

$$U^{\mathrm{VdW}}(r) = -J_{\mathrm{VdW}}.(\sigma/r).\exp\big(-(r - \sigma)/d\big) \quad r > \sigma \tag{14}$$

with J_{VdW} (in $k_B T$ units) and d (in Å), respectively, the depth and the range of the potential.
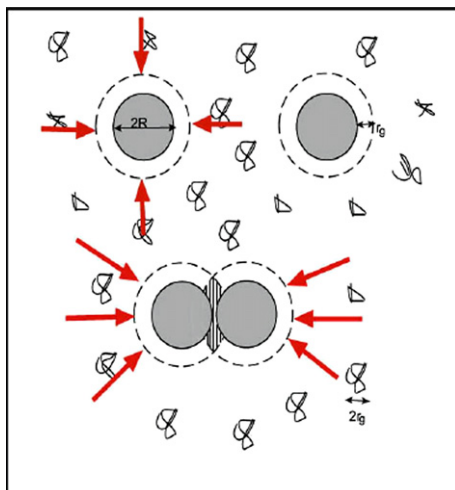
Fig. 2. Schematic representation of the depletion effect in a polymer–protein mixture.

In the DLVO potential, hard-sphere and electrostatic interactions have a repulsive effect which favors solubility. Except at pI where they dominate and may lead to precipitation rather than to desired crystallization, the van der Waals forces are weaker (or even disappear) than the coulombic interactions. It is therefore clear that the basic interactions considered in the DLVO potential model are generally unable to provide the attraction necessary for macromolecular nucleation and crystal growth. Fortunately, other forces can play a role, such as the attraction due to salt addition and/or the depletion attraction.

2.3. The Hofmeister effect

Salt has long been known to act as a crystallizing agent [23]. A number of phase diagrams were measured [24,25] and showed that solubility varies with the type of salt, following the direct/reverse order of the Hofmeister series according to whether the macromolecules are studied at a pH higher/lower than the pI, respectively. The effect of monovalent salts on protein interactions in solution was analyzed as a function of the particle size. With small macromolecules, monovalent anions were observed not only to screen the charges, but to induce an additional attraction, specific to salt type [3,26]. This attraction is short-range, about 3 Å, and its depth increases with decreasing temperature. With increasing molecular weight macromolecules, the Hofmeister effect (the salt-induced attraction) is sometimes found not sufficient to induce crystallization, the range being too short to allow attraction between macromolecules [13,14,27]. To circumvent this unfavorable effect on large macromolecules, non-adsorbing polymers can therefore play a role in attraction and crystallization.

2.4. The depletion attraction

The addition of neutral non-interacting polymers to colloids in solution has long been known to induce a depletion attraction [15]. This depletion interaction can be explained in a simplified manner for an ideal polymer solution effect in a protein–polymer mixture (Fig. 2).

Molecules of polymer — characterized by their radius of gyration R_g — and proteins (R) cannot mutually interpenetrate, and furthermore, the center of polymers is excluded from a region of thickness R_g around each protein. This excluded volume is called the depletion zone. When two proteins come sufficiently close to each other, their depletion zones overlap and the free volume accessible to the polymer molecules increases, leading to a gain in entropy of the system. Thermodynamically, it is therefore more favorable for the polymer when proteins approach each other, i.e. when there is an attractive interaction between them. This model remains valid as long as polymer molecules do not overlap. To describe the direct polymer–polymer potential $U_{\text{pol-pol}}(r)$, we used an approach where the effective potential is finite for all distances between two polymer molecule centers of mass. Molecules of polymer were therefore considered as "soft colloids". The mathematical form chosen for the polymer–polymer potential was a Gaussian form [28]:

$$U_{\text{pol-pol}}(r) = J_{\text{pol}} \cdot \exp\left(-(r/R_{\text{pol}})^2\right) \tag{15}$$

where J_{pol} (in $k_B T$ units) and R_{pol} (in Å) are the prefactor parameter and the range of the Gaussian potential respectively.

For the direct protein–polymer potential $U_{\text{pol-prot}}(r)$, we also chose a Yukawa form, which depends on only two parameters, the intensity $J_{\text{pol-prot}}$ (in $k_B T$ units) and the range of the potential $d_{\text{pol-prot}}$ (in Å).

$$U_{\text{pol-prot}}(r) = \begin{cases} +\infty & r \leqslant \sigma/2 \\ J_{\text{pol-prot}} \cdot \frac{\sigma}{2r} \cdot \exp(-(r-\sigma/2)/d_{\text{pol-prot}}) & r > \sigma/2 \end{cases} \tag{16}$$

Thus, the numerical simulations provide us with an effective macromolecule–macromolecule potential, $U_{\text{prot-prot}}^{\text{eff}}(r)$, which may be written as the sum of the macromolecular interaction potential in the absence of polymer, $U_{\text{prot-prot}}(r)$, and of the depletion term, $U_{\text{depletion}}(r)$:

$$U_{\text{prot-prot}}^{\text{eff}}(r) = U_{\text{prot-prot}}(r) + U_{\text{depletion}}(r) \tag{17}$$

Finally, we characterized the main pair potentials that control macromolecule distribution and thus solution properties. The electrostatic pair potential controls the macromolecule solubility. Indeed pH, by modifying the protein net charge, enables the modulation of repulsion, leading to an increase in the solubility. Then salt, by screening protein charges, induces a decrease in repulsion and at high salt concentration a possible increase in attraction leading to a decrease in solubility and therefore to crystallization. Finally non-adsorbing polymer induces a depletion attraction, which varies both with polymer size and with polymer concentration and which can also lead to crystallization. The electrostatic coulombic forces vary from a few Å up to some nm. Salt induces a short-range attraction, whereas polymer induces a short to medium-range potential. By choosing the appropriate pH, salt in the Hofmeister series as well as polymer concentration and size, it is possible to modify the phase diagram and thus control protein crystallization. But other effects can be involved in the control of potentials and phase diagrams. Surprisingly, recent results suggest that the addition of salt can induce an increase in repulsion instead of an increase in attraction. Most articles generally report that addition of salt decreases solubility, which is correlated with the fact that salt induces attractive interactions through charge screening. This effect, known as salting-out [23], is generally observed at medium and high salt concentrations. At low ionic strength, the opposite effect is expected, i.e. salting-in, where solubility increases with addition of salt. This salting-in effect, which is sporadically reported [29], has been observed with a therapeutic enzyme, urate oxidase. A cation binding on specific urate oxidase sites, similar to what was recently reported [30], allows us to explain the change in solubility and to design specific phase diagram with low or high solubility, which finds its interest in specific applications. In addition to this cation-binding effect, we characterized with urate oxidase a double effect of amphiphilic poloxamers, a solubilising agent at low concentrations, below the critical micellar concentration (cmc), and a precipitating agent at high concentrations above cmc, which makes these polymers useful in pharmaceutical applications.

In this review we will therefore describe how salt binding or amphiphilic polymers modify the different interaction forces in the special case of urate oxidase and finally how phase diagrams via solubility curves can be modulated to design crystals for different applications (bio-crystallography, or pharmaceutical processes for example).

2.5. Urate oxidase, a therapeutic model for crystallogenesis

Lysozyme has long been used as model protein to study nucleation and crystal growth mechanisms [31–34], since it is easily available at low cost. We used urate oxidase from *Aspergillus flavus* as a new therapeutic model system (Sanofi, France) in order to elucidate its catalytic mechanism, develop a new purification process and open new routes for protein crystallization in general. Urate oxidase is used as a protein drug to reduce toxic uric acid accumulation and to treat the hyperuricemic disorders occurring during chemotherapy. Urate oxidase *from Aspergillus flavus* is produced, purified and made commercially available by Sanofi (France). It is normally purified using multiple steps of concentration and chromatography. However, it could be purified by crystallization [35]. Crystallization has the inherent advantages of providing higher final purity yields, not denaturing the protein of interest and often providing some stabilization effects, but it requires a good knowledge of the phase diagram and a substantial amount of the protein to be crystallized. However, crystallization of proteins is mainly used to solve 3D structures at atomic level by X-ray or neutron diffraction. The first X-ray structure of urate oxidase was solved at 2.2 Å resolution from crystal grown in sodium carbonate pH 10.5 without precipitant agent after six months in cold room [36]. After this spontaneous crystallization, it appeared necessary to control crystallization in time and temperature. Characterization of new crystallization conditions via second virial coefficient measurements [12,37, 38] made it possible resolution of crystallographic structures of urate oxidase in the absence as well as in the presence of different inhibitors at high resolution from 1.7 to 1.0 Å resolution [39–43]. Polyethylene glycols clearly appeared as suitable crystallizing agents to rapidly grow urate oxidase diffracting crystals at room temperature. Although different urate oxidase structures were determined, its catalytic mechanism was not completely understood. High pressure crystallography could be a suitable technique to bring new information on structural changes of the protein, but this technique requires stable crystals under pressure, well-defined in size and in a high symmetry space group.

In both cases, purification by crystallization or high pressure crystallography, obtaining the right protein crystal requires determination of appropriate phase diagrams, which can be achieved by a good knowledge of solution properties.

3. Results and discussion

3.1. Cation binding effect

Urate oxidase is a homotetrameric enzyme, stable at pH above 7 up to 10.5 and instable at acidic pH, where it may dissociate into dimers. Its theoretical isoelectric point (pI), calculated from its primary structure and the pK_a of each charged amino acid, is about 7.0–7.5. In a buffer at pH close to pI without any crystallizing agents, the protein net charge is close to zero. There is no electrostatic repulsion. Usually protein solubility is minimum at pI [44], and van der Waals attraction
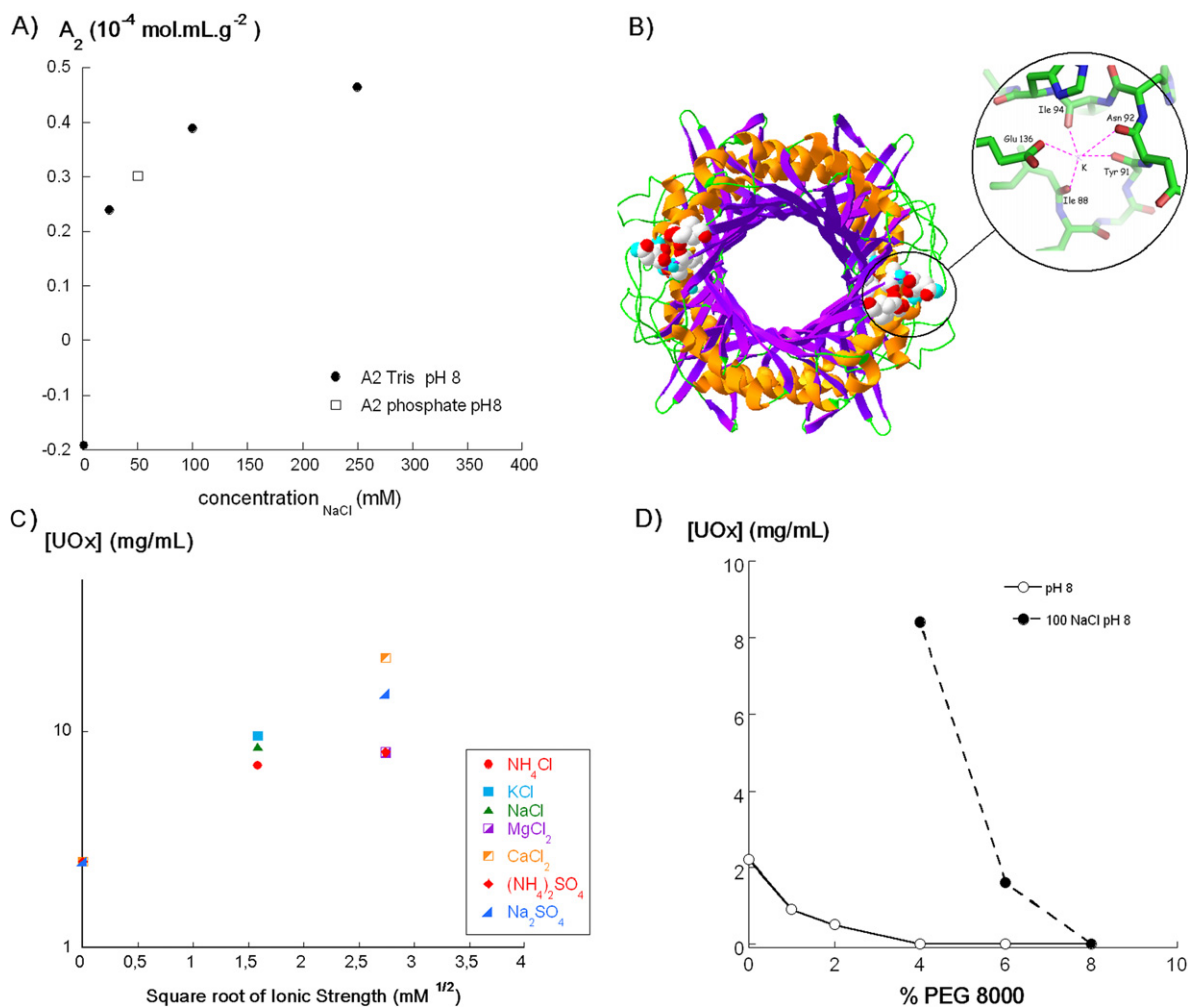
Fig. 3. A) Variation of A_2 in Tris buffer pH with addition of sodium chloride. B) Cationic binding site on the urate oxidase surface (courtesy of G. Marassio). C) Solubility of urate oxidase as a function of different salt concentrations. D) Solubility of urate oxidase as a function of PEG addition in the presence and absence of salt.

alone may induce their instability and aggregation. At pH above pI, where it is stable, the urate oxidase negative net charge increases as pH increases. Urate oxidase electrostatic repulsions are expected to increase, which was confirmed (not shown here) from a compilation of second virial coefficient (A_2) values determined as a function of pH, from SAXS experiments [12,37,45]. Surprisingly, in phosphate buffer at pH 8, as pH approaches pI, A_2 remains positive, which is inconsistent with pure van der Waals attraction at pI and not consistent with the negative second virial coefficient measured in Tris buffer at the same pH 8 without addition of salt (Fig. 3A). This is due to residual charges on the protein brought by cations in the sodium phosphate buffer and confirmed by the increase in the second virial coefficient as sodium chloride concentration increases.

This result suggests that the addition of sodium salt, in particular by addition of cations, induces an increase in repulsion ($A_2 > 0$). Our result was highlighted by X-ray crystallography (Fig. 3B), which shows that the salting-in effect observed with urate oxidase at pH 8 in Tris buffer results from the direct binding of cations to specific sites (Colloc'h, personal communication) on the surface of the protein. A similar effect, which suggests that salting-in is induced by ion binding, was recently reported [30]. The salting-in effect is not specific to sodium cation, since it was also observed with other cations such as K$^+$, NH$_4^+$, Mg^{2+}, Ca^{2+} (Fig. 3C). In all cases, the addition of salt leads to positive A_2 values, an indicator of repulsive interactions with urate oxidase, leading to an increase in solubility. Finally, the positive A_2 values of urate oxidase in sodium phosphate pH 8 or Tris buffers with some millimolars of salt are consistent with the high solubility of the protein and the negative A_2 value found in Tris buffer pH 8 without salt is consistent with attraction leading to crystallization of urate oxidase. Furthermore, at pI or close to pI, regardless of whether salt is present in the buffer (Tris pH 8 in our case), the addition of PEG to urate oxidase solutions induces attraction and leads to a decrease in solubility (Fig. 3D). However, at pH 8 the solubility of urate oxidase without salt in the buffer is lower than the solubility of urate oxidase with salt. Since nucleation and crystal growth are driven by the supersaturation β, with β the ratio [initial concentration]/[solubility],

a limited variation in solubility and therefore in supersaturation will be unfavorable to the growth of large crystals, favoring instead the nucleation of small crystals. It appears that salt is the absolute key to modulating solubility curves and designing specific crystals.

### 3.2. Rational route for stable urate oxidase crystal growth

Studying proteins under high pressure is aimed to meet a wide range of objectives, from understanding the physical chemistry of protein interactions with water to practical applications in food processing [46]. Many proteins have been studied using a variety of techniques, which can be applied under high pressure such as spectroscopic techniques [47], NMR spectroscopy [48], as well as a wide range of scattering techniques such as static and dynamic light scattering, neutron scattering and X-ray crystallography [49,50]. Such high-pressure approaches are generally used to resolve problems implying macromolecule structural changes. Growing crystals for high pressure X-ray crystallography (HPMX) requires specific requests. As for any crystallographic study, it is necessary to obtain a reasonably large crystal, suited into the pressure cell dimensions, preferentially in a high symmetry space group. The crystal has to remain stable in its mother liquor under pressure. Indeed, the effect of pressure on protein nucleation and crystallization can vary widely. In some cases, increased pressure increases the nucleation rate [51], while in other cases, the protein solubility increases, decreasing the nucleation rate [52]. Pressure may affect solubility and therefore lead either to dissolution of a crystal or to secondary nucleation. To circumvent the pressure effect on secondary crystal nucleation in the cell, the crystal must be placed in mother liquor containing no protein (low solubility in equilibrium with the crystal) and a high concentration of crystallizing agent, since variations in solubility caused by pressure are known to be reduced by increasing the crystallizing agent concentration [53]. To grow a small number of large crystals rather than a large number of small crystals, low supersaturation β has to be achieved. To optimize urate oxidase crystallization conditions for HPMX, we first characterized the phase diagram without salt, i.e. the conditions where solubility is lowest, as a function of PEG percentage (Fig. 4A) and explore different crystal growth conditions by using the microbatch technique [54].

The urate oxidase crystals obtained without addition of salt as a function of PEG 8000 are of two different shapes: tabular crystals when the percentage of PEG is below 4% and plate-like crystals when PEG percentage is above 4% (Fig. 4B). Unfortunately, crystals obtained at the lowest solubility, i.e. when percentages of PEG are greatest, are not suitable for crystal diffraction studies, being too numerous and poorly faceted. A suitable tabular crystal grown at a lower PEG percentage was picked out and placed in a glass cell. According to the solubility curve in 50 mM Tris pH 8, urate oxidase is totally insoluble in a solution of more than 10% PEG 8000. To control the stability of the crystal, protein-free mother liquor (15% PEG 8000, 50 mM Tris pH 8.0) is added to the crystal. The solubility, i.e. the concentration of the protein solution Δc remaining around the picked-out crystal, being too high, this leads to a secondary nucleation around the crystal (Fig. 4C). Indeed, the remaining protein solution around the crystal diluted in the protein-free mother liquor is supersaturated and induces a new nucleation under pressure. The crystallization conditions must therefore be a compromise between solubility, which is sufficient to grow large crystals but not too high, so as to avoid secondary nucleation when the mother liquor is added. Therefore, to obtain a massive-habit crystal at high PEG percentage, we added 100 mM NaCl, despite the salting-in effect which increases solubility, and determined the new solubility curve as a function of PEG 8000 (Fig. 4D). Crystal habits became more suitable for crystal diffraction studies (Fig. 4E, F) with sizes compatible with the pressure cell dimensions. We successfully transferred a crystal grown in 3.2 mg/mL of urate oxidase 6% PEG 100 mM NaCl Tris 50 mM pH 8 into a solution of 15% PEG 8000, 100 mM NaCl, 50 mM Tris pH 8.0. It remained stable for more than one week without secondary nucleation appearing. At this concentration of protein, no micro-crystals were generated from the solution surrounding the crystal, whereas at lower PEG and higher protein concentrations in the surrounding solution, many micro-crystals grew. HMPX experiments were then performed on the ID27 beamline on the European Synchrotron Radiation Facility (Grenoble, France) [55].

3.3. A new crystallizing agent

In some applications, for example in pharmaceutical processes, neutral polymers cannot be used because of their compatibility and toxicity. Polymers such as amphiphilic multi-block polymers are used in the cosmetic and pharmaceutical industries, more often as emulsifiers, solubilizers, dispersing and wetting agents in the preparation of solid dispersions than as crystallizing agents in bio-crystallography or in crystallization processes. We characterized a new class of crystallizing agent, the poloxamers, for soluble protein crystallization, compatible with both pharmaceutical processes and high-resolution structure determination in bio-crystallography. Poloxamer P188 is already used as a surfactant in the resuspension buffer for the solubilisation of lyophilized urate oxidase prior to administration. To date, its use as a crystallizing agent has never been described. It is a non-ionic co-polymer surfactant with a tri-block structure, composed of two hydrophilic segments, poly(oxyethylene) (PEO), and a central hydrophobic segment, poly(oxypropylene) (PPO), linked by ether bonds. The resulting construct can be represented as $HO(C_2H_4O)_a(C_3H_6O)_b(C_2H_4O)_aH$, where a is about 75 and b is about 31 [56] (Fig. 5). Its average molecular weight is around 8400 g mol^{-1} and its cmc (critical micellar concentration) is about 0.1% w/v [57]. Poloxamer is similar to the usual crystallizing agent for urate oxidase, PEG 8000, which is a linear hydrophilic polymer consisting of approximately $n = 180$ poly(oxyethylene) units and has a molecular weight of about 8000 g mol^{-1}.
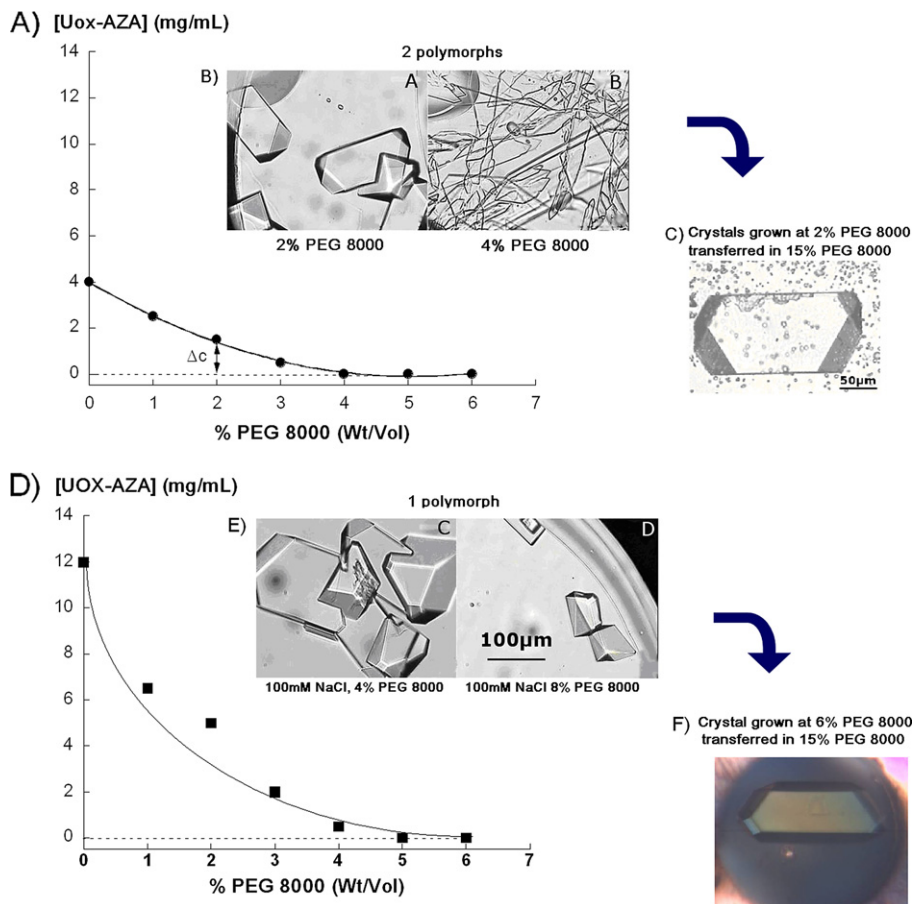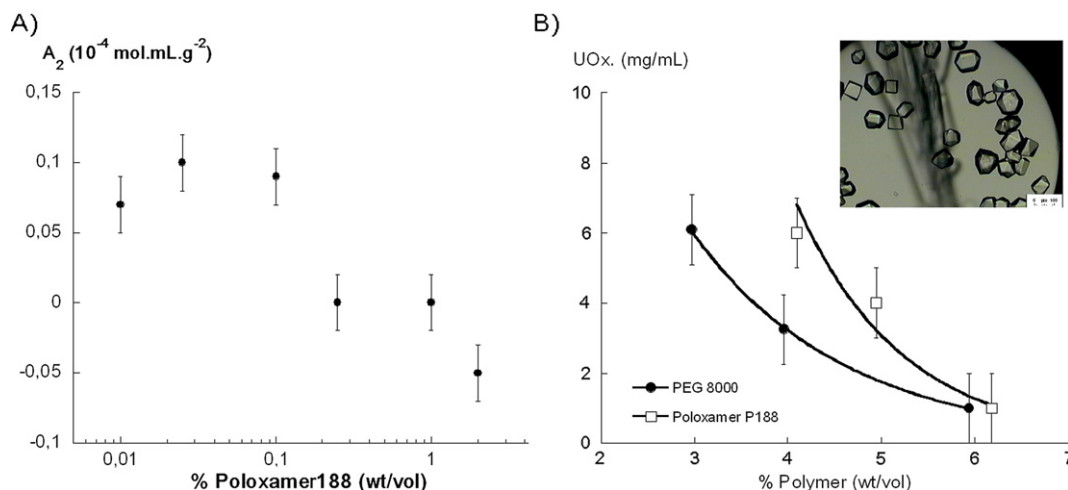
Fig. 4. A) Solubility of urate oxidase complexed with 8-azaxanthine, in Tris buffer pH 8, without salt, as a function of PEG 8000; B) Micrographs of urate oxidase crystals grown in microbatch at two PEG percentages; C) Micrograph of urate oxidase crystals transferred in 15% PEG 8000; D) Solubility of urate oxidase complexed with 8-azaxanthine, in Tris buffer pH 8, with 100 mM NaCl, as a function of PEG 8000; E) Micrographs of urate oxidase crystals grown in microbatch at two PEG percentages; F) Micrograph of urate oxidase crystal transferred in 15% PEG 8000.
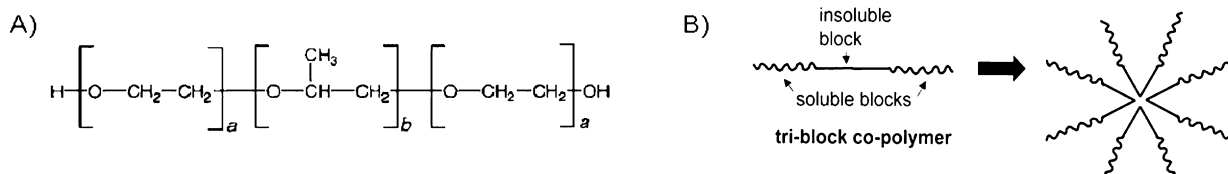
Fig. 5. A) Chemical structure of poloxamer P188, B) Scheme of micellization of poloxamer at $c >$ cmc ($\sim 0.1\%$).

Because of their amphiphilic structure, poloxamers have surfactant properties that make them useful in pharmaceutical applications. They can be used to increase water solubility of hydrophobic, oily substances as well as to increase the miscibility of two substances with different hydrophobicities. They were also used as model systems for drug delivery [58] applications. Recently, they have been shown to function as artificial chaperones to facilitate refolding of denatured proteins in solution or to suppress aggregation. In general, all these applications require low concentrations of poloxamer, typically below its cmc, involving monomeric poloxamer in solution. Below the cmc, the hydrophobic segment of polymer can non-specifically interact with exposed hydrophobic domains, preventing aggregation and aiding in the refolding of proteins [59]. However, high concentrations of poloxamer have also been reported to induce protein aggregation [60]. This suggests that it would be possible to use high concentrations of poloxamer to induce protein crystallization. To this end, we explored the interactions and crystallization of urate oxidase by addition of poloxamer P188. The second virial coefficient is positive without poloxamer in Tris pH 8 with 30 mM KCl, as expected from previous salting-in studies, and increases as the concentration of poloxamer increases up to its cmc (about 0.1%) (Fig. 6A). Above cmc, A_2 decreases and becomes negative at concentrations higher than 1%. Solubility of urate oxidase was therefore measured in the same conditions, as a function of concentration of poloxamer P188. As with PEG 8000, solubility decreases as the concentration of poloxamer increases

Fig. 6. A) Second virial coefficient of urate oxidase in solution as a function of % poloxamer P188. B) Comparison between solubility of urate oxidase in PEG 8000 and poloxamer P188 in 30 mM KCl, 50 mM Tris pH 7.5 at 20 °C, with urate oxidase crystal in poloxamer in insert.

above its cmc and is higher with poloxamer P188 than with PEG 8000 for concentrations lower than 6% (Fig. 6B). Thus, the surfacting or crystallizing nature of poloxamer P188 depends on its concentration. Below 0.1%, i.e. its cmc, poloxamer is monomeric. In this range of concentrations, it is possible that the hydrophobic central PPO block non-specifically interacts with solvent-exposed hydrophobic patches at the protein surface, while the hydrophilic surfactant chains remain exposed to the aqueous phase, increasing the solubility and the repulsion of urate oxidase. Above 0.1% poloxamer, micelles can form. The attractive effect of poloxamer at concentrations above 1% can be explained by a depletion effect driven by poloxamer micelles.

Crystals obtained in poloxamer P188 were tested for diffraction on the beamline FIP-BM30A at ESRF (Grenoble, France) and were found to diffract up to 1.6 Å [61]. We thus showed that poloxamer routinely used as a surfactant in pharmaceutical industry can also be used as crystallizing agent. But could it be used to purify urate oxidase by crystallization?
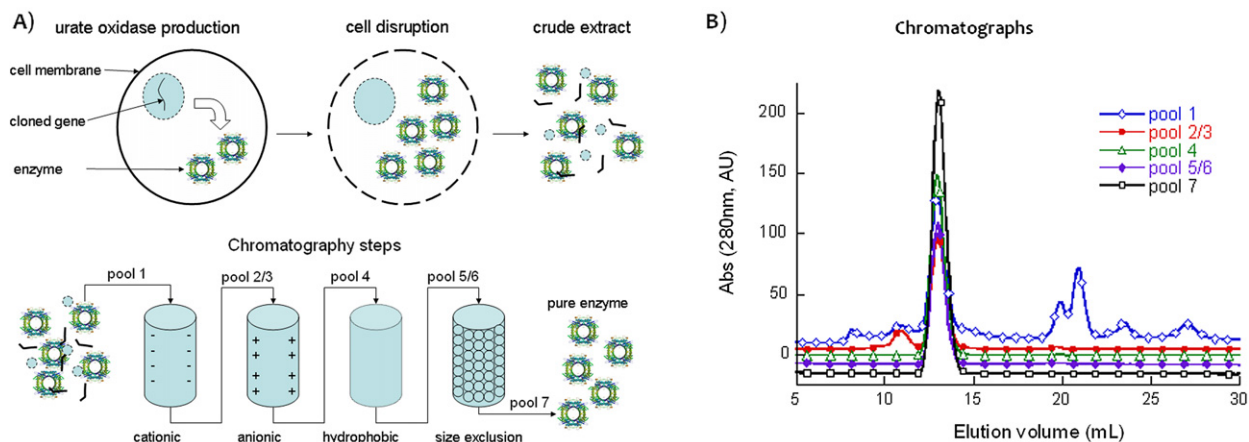
3.4. Urate oxidase purification by crystallization

Urate oxidase is currently produced in *Saccharomyces cerevisiae,* purified via four standard steps of chromatography (ion exchange, hydrophobic and gel filtration) (Fig. 7A). The different steps of the current process were analyzed by size exclusion chromatography (SEC) (Fig. 7B), isoelectrofocusing (IEF) and activity assays. The pool 1 chromatograph, which is the crude extract analysis, shows a main peak for urate oxidase (135 kDa) and impurities which are mainly aggregates with sizes higher than 670 kDa, large proteins of roughly 230 kDa, probably urate oxidase octamers (assessed by activity assay) and several unidentified host cell proteins or degradation products of molecular weights lower than 135 kDa. Pools 2/3 from the first chromatography, increases the urate oxidase purity up to 85%. The 15% of impurities remaining consist mainly of urate oxidase octamers. The second chromatography, which yields pool 4, purifies the urate oxidase further up to 99%. The last two chromatography steps are polishing steps. Implementing a crystallization step in this purification process would have industrial advantages if introduced after the first chromatography step (on pool 2/3), or preferably just before the first chromatography step (on pool 1).

We therefore tested the salting-in effect and the surfactant effect of poloxamer for urate oxidase purification on the most interesting steps, pool 1 and pool 2/3. First, poloxamer 188, above its cmc, was added to urate oxidase pool 1. In pure solution of active urate oxidase (pool 7), 100 μm well-defined crystals were previously grown by addition of poloxamer [61]. In pool 1, a solid form was obtained, but it appeared more like a precipitate than a crystal (Fig. 8A). The dissolved precipitate was analyzed by SEC (Fig. 8A), which showed that the process was not as effective as the current chromatography step 1. Aggregates could not be removed, while a decrease in proteins of low molecular weight was observed. Crystallization trials were then performed using reverse salt dialysis (i.e. dialysis against the same buffer without salt) on urate oxidase pool 1. In pure urate oxidase solution, well-defined 50 μm-sized crystals have previously been obtained in this way [45].

Here, 10 μm-sized solid forms were obtained. These are not as well shaped as pure crystals, but they no longer appear like precipitates (Fig. 8B). Analyzed by SEC, dissolved crystals showed fewer impurities than in pool 1 by poloxamer, both for high molecular weight and low molecular weight molecules (Fig. 9B). The overall purity of the urate oxidase obtained by reverse salt dialysis on pool 1 is comparable to what is obtained with the current step 1 (Fig. 7).

To explain why adding poloxamer was not an effective purification process for urate oxidase, the same procedure was performed on pool 2/3, i.e. partially purified urate oxidase containing the active form (tetramer) and aggregates likely to be urate oxidase octamers. Poloxamer 188 was added to urate oxidase pool 2/3. 10 μm-sized solid forms were obtained, not as well-shaped as crystals and appearing more like precipitates (Fig. 8C). These solid forms were separated from the

Fig. 7. A) Scheme of urate oxidase purification process. B) Size exclusion chromatography analysis of the 5 urate oxidase pools from the downstream process.
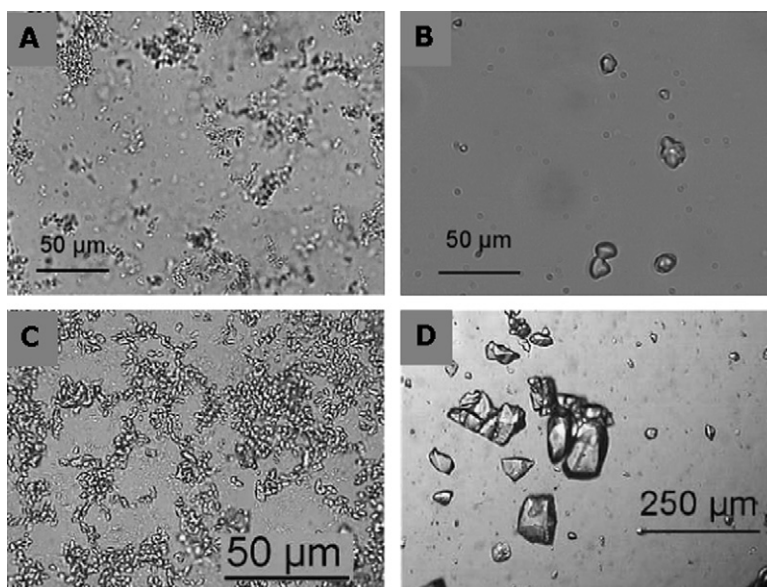

Fig. 8. Crystallization trials of urate oxidase from pool 1 and 3. Top) Crystallization conditions of pool 1. A) $c_{UOx} \approx 35$ mg/mL, 5% poloxamer 188, NH$_4$Cl 20 mM, Tris 5 mM pH 8.5. B) $c_{UOx} \approx 40$ mg/mL, Tris 5 mM pH 7.5, 20 mM NH$_4$Cl vs. Tris 5 mM pH 7.5. Bottom) Crystallization of pool 3. C) $c_{UOx} \approx$ 11 mg/mL, 2.5% poloxamer 188, NH$_4$Cl 45 mM, Tris 50 mM pH 7.5. D) $c_{UOx} \approx 68$ mg/mL 100 mM NH$_4$Cl, Tris 50 mM pH 7.5 vs. Tris 50 mM pH 7.5.

supernatant by centrifugation and the supernatant was pipetted. Solid forms were redissolved, and analysis of the solution by SEC, which showed that all impurities (octamers) are retained and that the process is ineffective (Fig. 9B). A second crystallization trial was performed using reverse salt dialysis of pool 2/3. 50 µm-sized well-shaped crystals were obtained (Fig. 8D). These crystals were separated from the supernatant by centrifugation and the supernatant was pipetted. Crystals were redissolved, and the solution analyzed by SEC, which showed fewer impurities (octamers) than in pool 2 (Fig. 9B). The overall purity of the urate oxidase obtained by reverse salt dialysis enables a decrease in octamer concentration, but is not as effective as the current second chromatography step. These experiments confirm that adding poloxamer is less effective than reverse salt dialysis for purifying urate oxidase. Urate oxidase octamers and other type of aggregates seem to be as sensitive as urate oxidase to the depletion effect induced by polymer, thus explaining its lack of selectivity. Moreover, the strong salting-in effect exhibited by urate oxidase seems to be absent in other types of aggregates and host cell proteins, which explains how purification can be achieved by this means.

4. Conclusion

Crystallization of proteins in solution is governed by an appropriate combination of interaction potentials in solution. Three main physico-chemical parameters or additives appear to play a crucial role in pair potentials: pH to modulate electrostatic repulsions, salt to induce repulsion by salting in effect or attraction by screening of protein charges and polymers
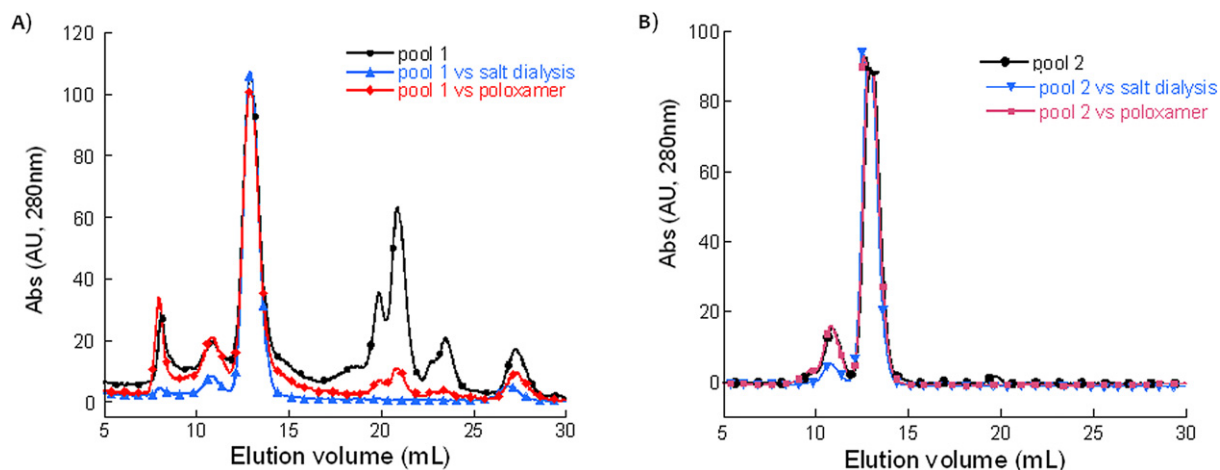
Fig. 9. SEC analysis of the urate oxidase crystal content A) from pool 1 compared to B) from pool 2/3. Crystallization conditions were for A) 35 mg/mL urate oxidase with 5% poloxamer 188 in 5 mM Tris pH 8.5, 50 mM NH_4Cl (red); 40 mg/mL urate oxidase in 5 mM Tris pH 8.5, 50 mM NH_4Cl, dialyzed against Tris 5 mM pH 8 (blue); B) 11 mg/mL urate oxidase with 2.5% poloxamer 188 in 5 mM Tris pH 8.5, 50 mM NH_4Cl (red); 68 mg/mL urate oxidase in 5 mM Tris pH 8.5, 50 mM NH_4Cl, dialyzed against 5 mM Tris pH 8 (blue). (For interpretation of the references to color in this figure legend, the reader is referred to the web version of this article.)

to induce depletion attraction. The design of small crystals or large diffracting crystals thus results from a subtle mix of strong or weak repulsions and attractions, which control the position of the solubility curve and the metastable zone in the phase diagram. We have shown with the example of urate oxidase that it is possible, via second virial coefficient measurements, to limit the number of trials for a first screening of crystallization conditions, and that knowledge of the effects of physico-chemical parameters on pair potentials will rationalize crystallization and crystal growth. We hope that these studies will help crystallographers and crystal growers in their quest for a rational route towards the crystallization of a particular protein.

Acknowledgements

References

[1] N. Asherie, et al., Phase diagram of colloidal solutions, Physical Review Letters 77 (1996) 4832–4835.
[2] P.R. Ten Wolde, D. Frenkel, Enhancement of protein crystal nucleation by critical density fluctuations, Science 277 (1997) 1975–1978.
[3] A. Tardieu, et al., Proteins in solution: from X-ray scattering intensities to interaction potentials, Journal of Crystal Growth 196 (1999) 193–203.
[4] D. Vivares, et al., Catching the PEG-induced attractive interaction between proteins, The European Physical Journal E 9 (2002) 15–25.
[5] F. Bonneté, et al., Second virial coefficient: variations with lysozyme crystallization conditions, Journal of Crystal Growth 196 (1999) 403–414.
[6] A. George, W.W. Wilson, Predicting protein crystallization from a dilute solution property, Acta Crystallographica D 50 (1994) 361–365.
[7] M. Muschol, F. Rosenberger, Interactions in under- and supersaturated lysozyme solutions. Static and dynamic light scattering results, Journal of Chemical Physics 103 (1995) 10424–10432.
[8] F. Vérétout, et al., Molecular basis of eye lens transparency. Osmotic pressure and X-ray analysis of alpha-crystallin solutions, Journal of Molecular Biology 205 (1989) 713–728.
[9] M. Malfois, et al., A model of attractive interactions to account for liquid–liquid phase separation of protein solutions, Journal of Chemical Physics 105 (1996) 3290–3300.
[10] D. Vivares, F. Bonneté, Liquid–liquid phase separations in urate oxidase/PEG mixtures: characterization and implications for protein crystallization, Journal of Physical Chemistry B 108 (2004) 6498.
[11] A. Ducruix, et al., Protein interactions as seen by solution X-ray scattering prior to crystallogenesis, Journal of Crystal Growth 168 (1996) 28–39.
[12] D. Vivares, F. Bonneté, X-ray scattering studies of Aspergillus flavus urate oxidase: towards a better understanding of PEG effects on the crystallization of large proteins, Acta Crystallographica D 58 (2002) 472–479.
[13] S. Finet, A. Tardieu, Alpha-crystallin interaction forces studied by small angle X-ray scattering and numerical simulations, Journal of Crystal Growth 232 (2001) 40–49.
[14] M. Budayova, et al., Interactions in solution of large oligomeric protein, Journal of Crystal Growth 196 (1999) 210–219.
[15] S. Asakura, F. Oosawa, On the interaction between two bodies immersed in a solution of macromolecules, Journal of Chemical Physics 22 (1954) 1255–1256.
[16] A. Guinier, G. Fournet, Small Angle Scattering of X-Rays, Wiley, New York, 1955.
[17] W.G. Mcmillan, J.E. Mayer, The statistical thermodynamics of multicomponent systems, Journal of Chemical Physics 13 (1945) 276–306.
[18] B.H. Zimm, Application of the methods of molecular distribution to solutions of large molecules, Journal of Chemical Physics 14 (1946) 164–180.

[19] C. Haas, et al., Relation between the solubility of proteins in aqueous solutions and the second virial coefficient of the solution, The Journal of Physical Chemistry B 103 (1999) 2808–2811.

[20] L. Belloni, A hypernetted chain study of highly asymmetrical polyelectrolytes, Chemical Physics 99 (1985) 43–54.

[21] L. Belloni, Self-consistent integral equation applied to the highly charged primitive model, Journal of Chemical Physics 88 (1988) 5143–5148.

[22] L. Belloni, Interacting monodisperse and polydisperse spheres, in: T. Zemb, P. Lindner (Eds.), Neutron, X-Ray and Light Scattering, in: North-Holland Delta Series, Elsevier Science Publishers B.V., Amsterdam, Oxford, New York, Tokyo, 1991, pp. 135–155.

[23] T. Arakawa, S. Timasheff, Theory of protein solubility, Methods in Enzymology 114 (1985) 49–77.

[24] C. Carbonnaux, et al., Relative effectiveness of various anions on the solubility of acidic Hypoderma lineatum collagenase at pH 7.2, Protein Science 4 (1995) 2123–2128.

[25] J.-P. Guilloteau, et al., Variation of lysozyme solubility as a function of temperature in the presence of organic and inorganic salts, Journal of Crystal Growth 122 (1992) 223–230.

[26] S. Finet, et al., The Hofmeister effect as seen by SAXS in protein solutions, Current Opinion in Colloid & Interface Science 9 (2004) 112–116.

[27] M. Casselyn, et al., Spherical plant viruses: interactions in solution, phase diagrams and crystallization of brome mosaic virus, Acta Crystallographica. Section D. Biological Crystallography 57 (2001) 1799–1812.

[28] P.G. Bolhuis, et al., Accurate effective pair potential for polymer solutions, Journal of Chemical Physics 114 (2001) 4296–4311.

[29] C. Faber, et al., Study of the solubility of a modified bacillus licheniformis r-amylase around the isoelectric point, Journal of Chemical and Engineering Data 52 (2007) 707–713.

[30] C.L.D. Gibb, B.C. Gibb, Anion binding to hydrophobic concavity is central to the salting-in effects of Hofmeister chaotropes, Journal of the American Chemical Society 133 (2011) 7344–7347.

[31] J. Drenth, The nucleation of lysozyme from a fluctuation point of view, Crystal Growth & Design 5 (2005) 1125–1127.

[32] J.A. Gavira, J.M. Garcia-Ruiz, Effects of a magnetic field on lysozyme crystal nucleation and growth in a diffusive environment, Crystal Growth & Design 9 (2009) 2610–2615.

[33] Y.X. Liu, et al., Toward further understanding of lysozyme crystallization: phase diagram, protein–protein interaction, nucleation kinetics, and growth kinetics, Crystal Growth & Design 10 (2010) 548–558.

[34] P.G. Vekilov, Nucleation, Crystal Growth & Design 10 (2010) 5007–5019.

[35] C. Jacobsen, et al., Nucleation and growth of microbial lipase crystals from clarified concentrated fermentation broths, Biotechnology and Bioengineering 57 (1998) 666–675.

[36] N. Colloc'h, et al., Crystal structure of the protein drug urate oxidase-inhibitor complex at 2.05 A resolution, Nature Structural Biology 4 (1997) 947–952.

[37] F. Bonneté, et al., Interactions in solution and crystallization of Aspergillus flavus urate oxidase, Journal of Crystal Growth 232 (2001) 330–339.

[38] F. Bonneté, D. Vivares, Interest of the normalized second virial coefficient and interaction potentials for crystallizing large macromolecules, Acta Crystallographica D 58 (2002) 1571–1575.

[39] P. Retailleau, et al., Urate oxidase from Aspergillus flavus: new crystal-packing contacts in relation to the content of the active site, Acta Crystallographica D 61 (2005) 218–229.

[40] P. Retailleau, et al., Complexed and ligand-free high resolution structures of Urate oxidase (Uox) from Aspergillus flavus: a re-assignation of the active site binding mode, Acta Crystallographica D 60 (2004) 453–462.

[41] L. Gabison, et al., Near-atomic resolution structures of urate oxidase complexed with its substrate and analogues: the protonation state of the ligand, Acta Crystallographica D 66 (2010) 714–724.

[42] L. Gabison, et al., Structural analysis of urate oxidase in complex with its natural substrate inhibited by cyanide: Mechanistic implications, BMC Structural Biology 8 (2008).

[43] M. Budayova-Spano, et al., A preliminary neutron diffraction study of rasburicase, a recombinant urate oxidase enzyme, complexed with 8-azaxanthin, Acta Crystallographica F 62 (2006) 306–309.

[44] M. Riès-Kautt, A. Ducruix, From solution to crystals with a physico-chemical aspect, in: R. Giegé (Ed.), Crystallization of Nucleic Acids and Proteins – A Practical Approach, Oxford University Press, Oxford, New York, Tokyo, 1999.

[45] M. Giffard, et al., Salting-in effect on urate oxidase crystal design, Crystal Growth & Design 8 (2008) 4220–4226.

[46] R. Hayashi, et al., Introduction of high pressure to food processing: Preferential proteolysis of β-lactoglobulin in milk whey, Journal of Food Science 52 (1987) 1107–1108.

[47] K. Heremans, L. Smeller, Protein structure and dynamics at high pressure, Biochimica et Biophysica Acta 1386 (1998) 353–370.

[48] T.A. Jones, et al., Improved methods for building protein models in electron density maps and the location of errors in these models, Acta Crystallographica A 47 (1991) 110–119.

[49] R. Fourme, et al., High-pressure protein crystallography (HPPX): instrumentation, methodology and results on lysozyme crystals, Journal of Synchrotron Radiation 8 (2001) 1149–1156.

[50] R. Fourme, et al., High-pressure macromolecular crystallography (HPMX): status and prospects, Biochimica et Biophysica Acta 1764 (2006) 384–390.

[51] K. Visuri, et al., A new method for protein crystallization using high pressure, Nature Biotechnology 8 (1990) 547–549.

[52] B. Lorber, et al., Effect of high hydrostatic pressure on nucleation and growth of protein crystals, Journal of Crystal Growth 158 (1996) 103–117.

[53] M. Gross, R. Jaenicke, Growth inhibition of lysozyme crystals at high hydrostatic pressure, FEBS Letters 284 (1991) 87–90.

[54] N. Chayen, Protein crystallization, in: Structural Genomics and High Throughput Structural Biology, CRC Press, 2005, pp. 29–48.

[55] E. Girard, et al., Structure-function perturbation and dissociation of tetrameric urate oxidase by high hydrostatic pressure, Biophysical Journal 98 (2010) 2365–2373.

[56] Z. Takáts, et al., Qualitative and quantitative determination of poloxamer surfactants by mass spectrometry, Rapid Communications in Mass Spectrometry 15 (2001) 805–810.

[57] I. Schmolka, A review of block polymer surfactants, Journal of the American Oil Chemists' Society 54 (1977) 110–116.

[58] M. Adams, et al., Amphiphilic block copolymers for drug delivery, Journal of Pharmaceutical Sciences 92 (2003) 1343–1355.

[59] R.C. Lee, et al., Surfactant copolymers prevent aggregation of heat denatured lysozyme, Annals of Biomedical Engineering 34 (2006) 1190–1200.

[60] L.A. Garcia, Production of antisera comprising fractionating plasma or serum with an ethylene oxide-polyoxypropylene block copolymer, Baxter Laboratories, Inc., United States of America, 1975.

[61] M. Giffard, et al., Surfactant poloxamer 188 as a new crystallizing agent for urate oxidase, Crystal Growth & Design 9 (2009) 4199–4206.